A concept mission for the Stellar Population and Evolution with Cubesats (SPEC)

Giammarco Cialone[a,1,*], Andrea Gianfermo[a], Alessandra Di Cecco[e,1], Silvia Mari[c], Fabio Santoni[d], Fabrizio Piergentili[a]

[a]*Department of Mechanical and Aerospace Engineering, University or Rome La Sapienza, Via Eudossiana 18, Rome, Italy, 00185*
[b]*Physics Department, University or Rome La Sapienza, p.le Aldo Moro 5, Rome, Italy, 00185*
[c]*Agenzia Spaziale Italiana, Via del Politecnico snc, Rome, Italy, 00133*
[d]*Dipartimento di Ingegneria Astronautica, Elettrica ed Energetica, Via Eudossiana 18, Rome, Italy, 00185*
[e]*INAF-OAAb, Osservatorio Astronomico dAbruzzo, via Mentore Maggini snc, cap 64100 Teramo*

Abstract

Binary or multiple stellar systems, constituting almost half of the content of the Milky Way, represent a high priority astronomical target due to their repercussions on the stellar dynamical and evolutionary parameters. Moreover the spectral study of such class of stars allows to better constrain the evolutionary theories of the Galactic stellar populations. By directly observing the members of a stellar system we are able to perform more detailed spectrometric measurements and better infer their mass. In this paper we investigate the feasibility of a cubesat based mission including an optical payload to directly optically discriminate the members of a selected sample of binary systems. The scientific targets, consisting 124 M class dwarf stars binary systems, have been extracted from the already studied Riaz catalogue. These subset has been selected considering the star distance, the members angular separation, and the distance from the Galactic plane (due to limit the background and foreground contamination). The satellite concept is based on a 6 unit Cubesat embedding some commercial off the shelf components and an ad-hoc designed optical payload

*Corresponding author at: Department of Mechanical and Aerospace Engineering, University or Rome La Sapienza, Via Eudossiana 18, Rome, Italy, 0018
Email address: `giammarco.cialone@uniroma1.it` (Giammarco Cialone)

occupying almost 4 units. The optical configuration has been chosen in order to fit the angular resolution requirements, as derived from the target characteristics. Moreover, according to the optical analysis and the computed field of view some requirements on the attitude control system have been inferred and fulfilled by the component selection. The paper is organized as in the following: a brief scientific introduction is made; consequently the project is described with particular attention to the optical design and the standard sub-systems; finally the conclusions are drawn and the future perspectives are investigated.

Keywords: Cubesat, Optical payload, Stellar evolution

1. Introduction

1.1. Scientific context

Majority of stars populating the Milky Way is distributed in stellar systems with two or more members, gravitationally bounded and orbiting around a common centre of mass. A high percentage of these systems presents binarity, having two members. Respect to the total number of stars, the binary fraction ($N_{\text{binaries}}/N_{\text{total}}$) has been observed to decrease as a function of stellar mass [1]. In particular, observations suggest that this quantity ranges from 57% for the sun-like stars of class G to 26-42% for class M0-M6, and even lower values of 10-30% for very low mass stars (VLMSs) with $M < 0.1 M_\odot$ [2]. By studying the binary systems of the M-dwarf stars, several dynamical and evolutionary parameters can be addressed. In the investigation provided by Bergfors et al. (2010)[2], 124 M0-M6 young dwarf stars were selected from the Riaz catalogue, including more than 1000 objects lying within a 52 pc distance from us [3]. The choice of younger systems was made because of the easier detection of such warmer and brighter stars [4]. In fact the visual absolute magnitude of the M-dwarfs is approximately 10-16 mag and the effective temperature is of 2500-4000 K. These catalogue selected stars were investigated by studying their spectral type, observing the systems in the i' and z' Sloan Digital Sky Survey (SDSS) filters [5]. Bergfors et al. assumed a linear relation between the fluxes

and the integrated spectral type as done in Daemgen et al. (2007)[6], and the magnitude-spectral type relation obtained by the Spectral Energy Distribution (SED) fitting of M-dwarfs up to L0 class (Kraus & Hillenbrand 2007 [7]). The aforementioned investigation is based on high resolution data $(1'')$, but the small field of view (FoV) limits the study of binaries with angular distance $\theta > 6''$. By taking into account Bergfors et al. assumptions we proposed a preliminary study for a cubesat mission dedicated to M dwarf binaries observation.

1.2. Science with Cubesats

In the last decades the idea of developing smaller low-cost satellite, to perform mission usually performed by big satellites, has been repeatedly discussed by the space community. This idea materialized when the availability of a low cost launch alongside of bigger payload became possible. To exploit this opportunity, the standardization of the combination of deployer and satellite was the keystone to the success of CubeSats. CubeSats did not born as a standard, their goal was to allow students to be able to design and built a simple spacecraft. A CubeSat is defined as a nanosatellite composed by Units (U) of 10 cm x 10 cm x 10 cm for approximately 1.33kg each. The nanosatellite does not diverge much in design from bigger satellites as it include almost all the subsystems as Attitude Determination and Control (ADCS), Tracking Telemetry and Command (TT&C) and Electrical Power Subsystem (ESP). The primary goal of CubeSats is to provide a small, light-weight, low-cost platform for academic and technology demonstration. Over time the development of CubeSats became attractive also for scientific and commercial payload due to the increase of reliability of components and to the increase of number of Us, 6U and 12U CubeSats, being able to be launched. In such framework the Sapienza Space System and Space Surveillance Laboratory (S5Lab hereafter), founded in 2013 and hosted by the Univesity of Rome La Sapienza, realized several nanosatellite projects embedding payloads with scientific purpose. Among the most recent S5Lab projects there are: URSA MAIOR, launched in June 2017, consisting in a 3U Cubesat [8, 9] including the MEMS space propulsion experimental payload

[10]. This project was followed by the Italian Space Agency (ASI) supported project called 1KUNS, a 1U nanosatellite scheduled for launch in April 2018 and realized in collaboration with the Nairobi University. Furthermore, a 1U LED-based payload called LEDSAT has been approved and supported by the European Space Agency (ESA) and is currently being developed by the S5Lab team with a scheduled launch in 2020 [11, 12]. Finally, the SPEC nanosatellite, introduced in this paper, is currently being developed in the framework of the space observation to enhance low cost scientific research and to demonstrate the capability of compact optical payload on CubeSats.

2. The SPEC Project

2.1. Mission Concept

The SPEC mission based on a 6U Cubesat, has been conceived in order to study stellar binary systems with the maximum possible angular resolution on such a small payload dedicated volume. To this purpose, we selected 11 observational targets with $\theta > 10$" by using the binary catalogue provided by Ward-Duong et al. (2015)[13], based on the Hipparcos catalogue within a distance of 15 pc from the Sun (van Leeuwen 2007[14]). The targets, shown in fig. 1, were selected far from the Galactic Plane (galactic latitude higher than 15) in order avoid crowding contamination and as having a visual magnitude $V\mathrm{mag} \leq 12$. The optical payload system features have consequently been modelled around the selected mission targets as will be explained in section 2.2. Moreover, considering the homogeneously distributed targets of the mission, every LEO shall satisfy the mission scientific requirements. Therefore, the less constrained orbital parameters will surely result in an increased launch opportunity.

2.2. Optical Payload

The scientific optical payload of the SPEC 6U CubeSat,whose Cad design is represented in fig.2 consists of a small telescope. The chosen optical configuration is a standard Schmidt-Cassegrain, consisting in:
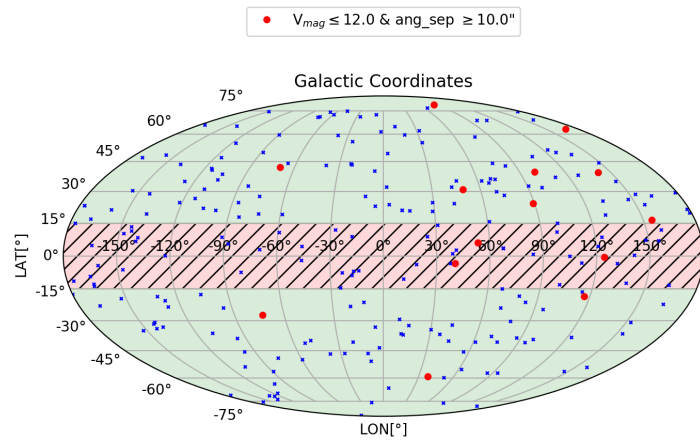
4

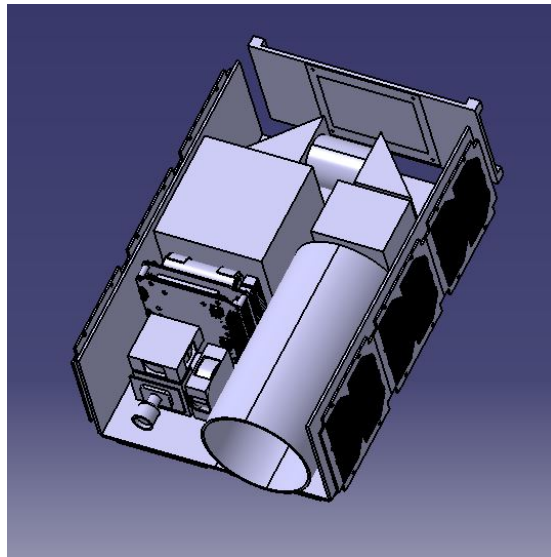Figure 1: SPEC selected targets, marked with red filled dots.

Figure 2: SPEC cad design.

- corrective Schmidt lens

- primary spherical mirror

- secondary convex mirror

In order to make the system as compact as possible the length of the optical tube has been fixed to a maximum of 17 cm. This length could be increased according to the total available volume in the satellite resulting in a higher focal length (which should result in a higher angular resolution). For the sake of simplicity all the optical model has been designed taking this dimension fixed and performing a double reflection of the ray beam in order to accomodate the sensor next to the optical tube. This has been done mainly because a single axis setup would have exceeded the maximum length of a 6U CubeSat of 32cm.

The tested optical system, described above and represented the fig. 3, is composed by:

- a corrective Schmidt lens whose internal surface has a 34483.79 mm curvature radius with 4th and 6th order coefficients in the sag $z(r)$ generic expression below of $-3.1977278 \times 10^{-9}$ and $1.2799361 \times 10^{-14}$. This optical element is also the aperture STOP of the system with an obstruction (represented by the secondary mirror diameter) of 16.65 mm radius, and a maximum radius of 44 mm

$$z(r) = \frac{r^2}{R\left(1 + \sqrt{1 - (1+k)\frac{r^2}{R^2}}\right)} + \alpha_4 r^4 + \alpha_6 r^6; \qquad (1)$$

- a primary spherical mirror of 90 mm diameter with a central hole of 16.65 mm and a curvature radius of -500 mm;

- a secondary aspherical mirror of 33.3 mm diameter, a curvature radius of -196.94 mm and a conic constant K of -0.96;

- a first fold mirror (with a 45 angle respect to the optical axis of the secondary mirror);

6

Table 1: SPEC optical elements position. Units are in mm.

Element	Absolute position	Position w.r.t. previous	Optical axis offset
Corrective lens	0	0	0
Primary mirror	176	176	0
Secondary mirror	5	-171	0
Fold mirror 1	237	232	0
Fold mirror 2	237	0	100
Sensor	192	45	100

- a second fold mirror (with a -45 angle respect to the optical axis of the secondary mirror and placed off axis respect to the optical tube);

- the focal plane on which the optical performances of the system are evaluated.

The position of the afore listed optical elements is reported in Table 1. The system should then be integrated with a filter which could both be active (liquid crystal filter) or passive (mounted on a filter wheel). The two selected filters for the mission should be the same as the i' and z' SDSS filters centred at 7625 and 9134 Angstroms. The filter pack should be inserted in the most feasible position in the optical chain out of the optical tube (volume enclosed between primary and secondary mirrors). Moreover, the filter system can be selected also according to the mission economic budget. An active liquid crystal filter pack which could guarantee narrower pass-bands and limit the mobile parts on the satellite or a passive filter wheel including standard filters can be included in the optical payload.

The optical performance analysis of the system has been performed with ZEMAX Optics Studio software, assuming an on axis FoV (Field of View) and four angled FoVs of 0.3 degree in the four symmetric directions of the object plane (the plane normal to the optical axis). The analysis has given the following results:

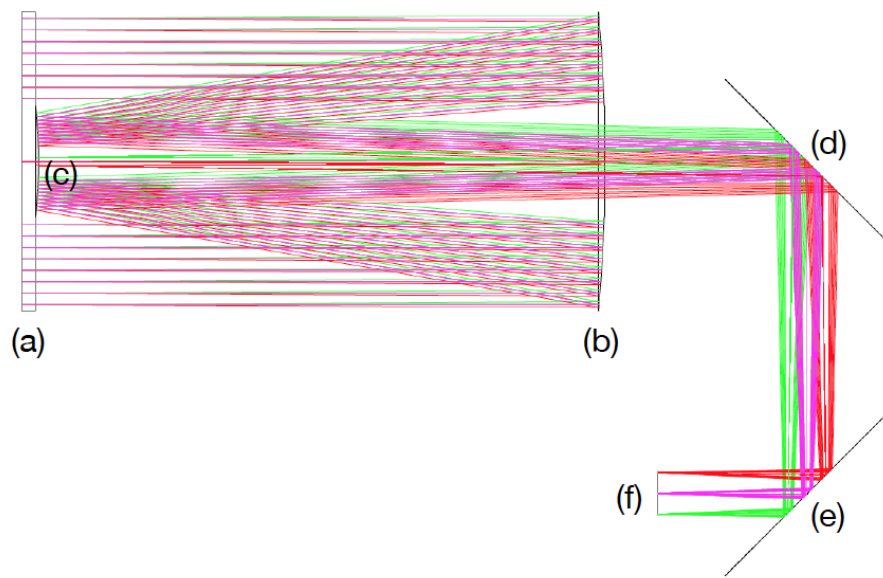- The spot diagram (SPT) from which we evaluate the distributions of the

Figure 3: SPEC optical design. In order: corrective Schmidt lens (a); primary spherical mirror (b); secondary aspherical mirror (c); first fold mirror (d); second fold mirror (e); camera sensor (f). The three different colours represent the 5 different analysed FoVs: green, purple, yellow and red rays represent the (0, -0.3), (0.3, 0), (-0.3, 0) and (0, 0.3) fields respectively; while the blue rays represent the optical axis aligned field (0, 0).
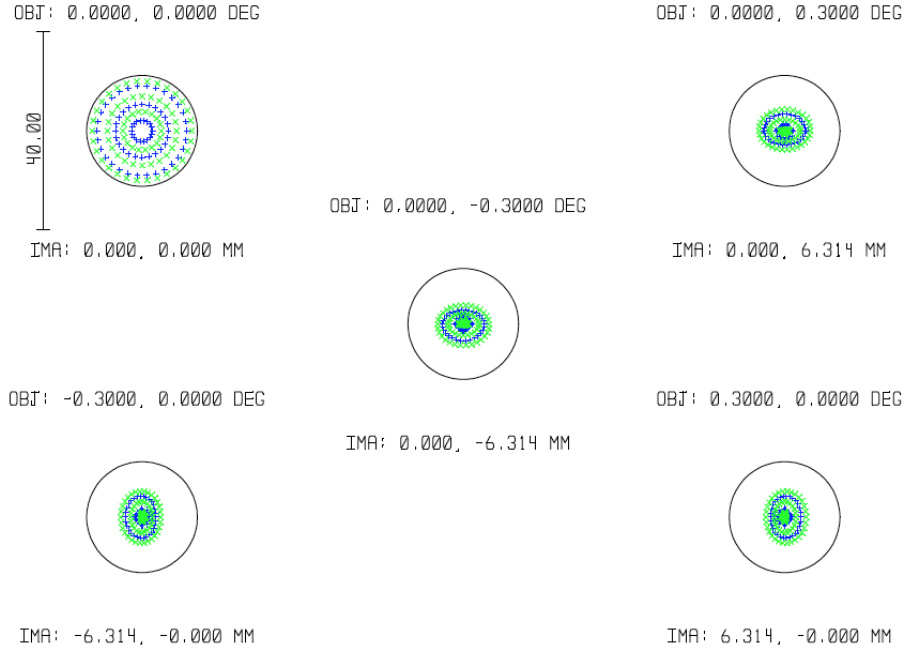
Figure 4: SPEC spot diagram for the five analysed FoVs. Black circles mark the Airy disk. Blue and green crosses represent the two considered wavelengths of the i' and z' filters respectively. In all the considered FoVs the radiation is distributed inside the Airy disk. Thus we qualitatively conclude the system satisfies the diffracion limit.

simulated light rays on the image plane (on the sensor) is shown in fig. 4. From this analysis we can extract the Airy disk diameter, which is of 22.45 microns and conclude that the distribution of the intensity on the focal plane is consistent with the diffraction limit requirement since the rays are inside the Airy disk.

- The encircled energy (EE), shown in fig. 5 is the second parameter from which we can verify the diffraction limited condition. This parameter represents the energy distribution from the chief ray (aligned with the selected FoV). From the energy distribution the first and second minimum of the Airy function are clearly identifiable (corresponding to the distribution plateau). Since the distributions for the different F0Vs are in good
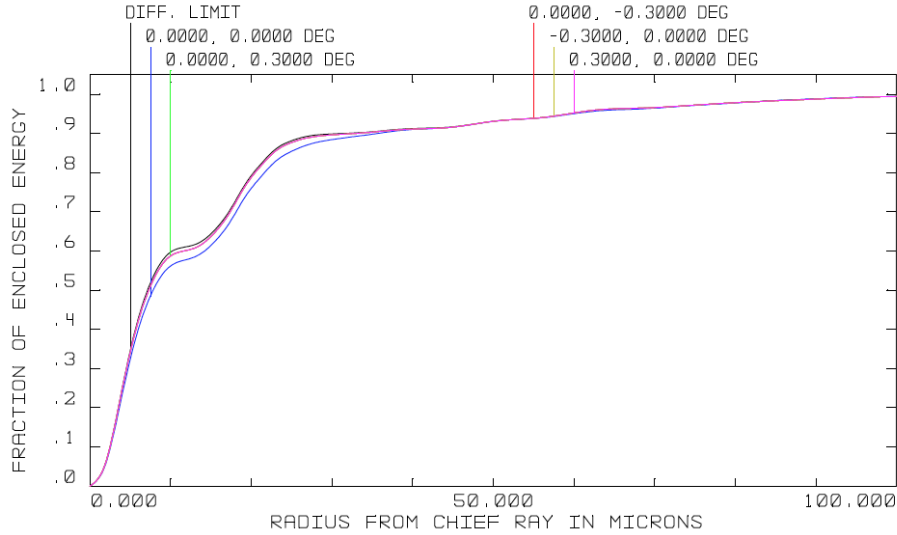
9

Figure 5: SPEC Encircled Energy (EE). Diffraction limit condition is reported in black solid line. The analysed FoVs are reported coloured solid lines instead. Being the realistic behaviours close to the diffracion limit we conclude that the system is diffraction limited.

agreement with the diffraction limit distribution we can conclude that the system satisfies the diffraction limited condition.

- The third optical analysis consists in the evaluation of the system modulus of the transfer function (MTF). This function is a figure of merit of the optical system which accounts for eventual aperture obstructions, diffractions and all considered system features. From the plot of the MTF, visible in fig. 6, we can deduce that the system satisfies the diffraction limited condition since the MTF is consistent with the diffraction limited theoretical one.

Thus we conclude that the optical performance of the system satisfies our required performance since it is diffraction limited. The available angular resolution θ of the system can be derived from the focal length f and the Airy disk
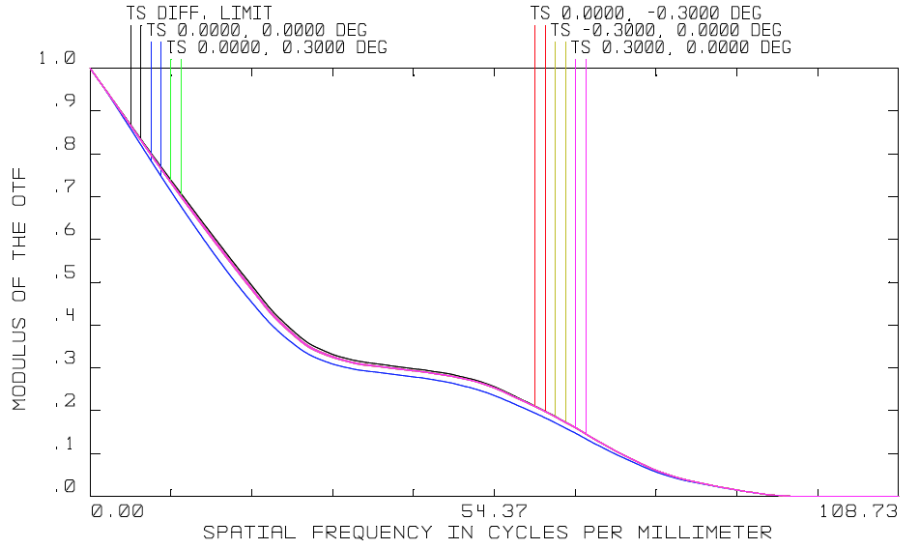
10

Figure 6: SPEC Modulus of the Transfer Function (MTF). The FoVs solid coloured lines agree with the diffraction limited behaviour. This confirms the system diffracion limited condition.

diameter d_{Airy} as reported below:

$$\theta = \arctan\left(\frac{d_{\text{Airy}}}{f}\right) \tag{2}$$

Moreover, since the focal length of the system corresponds to 1205643 microns and the Airy disk diameters for the two selected wavelength (i' and z' filters) are respectively 22.45 microns and 26.89 microns we can derive the two correspondent angular resolutions resulting in $\theta_{\text{i}'} = 3.84$" and $\theta_{\text{z}'} = 4.60$". Furthermore, following the same procedure, the optical system Field of View FoV_{sys} can be determined, considering the selected sensor dimensions d_{sens} and the focal length, as follows

$$\text{FoV}_{\text{sys}} = \arctan\left(\frac{d_{\text{sens}}}{f}\right). \tag{3}$$

Assuming a sensor able to take advantage of the full focal plane dimension the achieved FoV angle (as outputted from the optics design software) is $\simeq 0.6$.
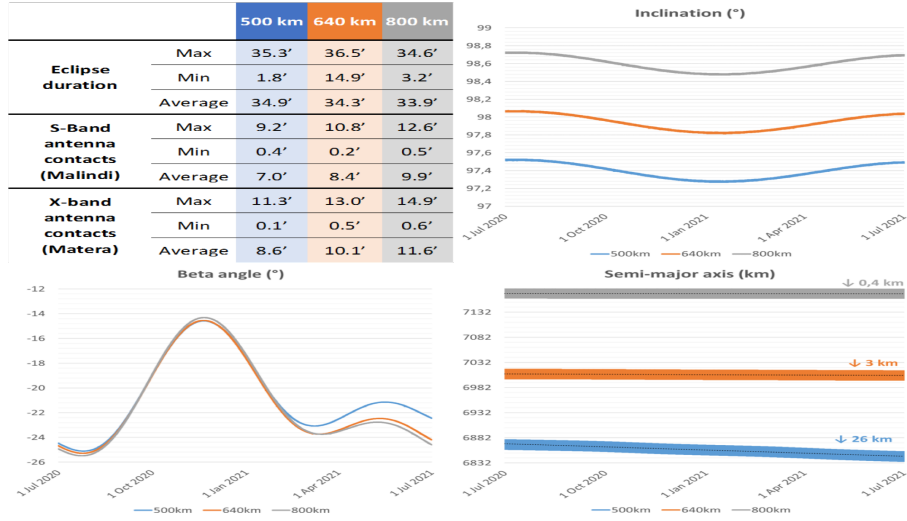
11

		500 km	640 km	800 km
Eclipse duration	Max	35.3'	36.5'	34.6'
	Min	1.8'	14.9'	3.2'
	Average	34.9'	34.3'	33.9'
S-Band antenna contacts (Malindi)	Max	9.2'	10.8'	12.6'
	Min	0.4'	0.2'	0.5'
	Average	7.0'	8.4'	9.9'
X-band antenna contacts (Matera)	Max	11.3'	13.0'	14.9'
	Min	0.1'	0.5'	0.6'
	Average	8.6'	10.1'	11.6'

Figure 7: SPEC orbital parameters and mission analysis results for the three different studied altitudes of 500, 640 and 800 kilometers.

2.3. Other subsystems

2.3.1. Mission Analysis

To achieve a periodic access to the Ground Stations (GS) network and a less variable thermal gradients due to solar irradiation, a Sun-Synchronous orbit (SSO) has been chosen. The homogeneous distributed binary stellar systems shall be scanned through the year due to the drift of the orbit. Three different orbit altitudes have been studied to cover a wide mission lifetime span and access time window intervals to the GSs. The results of the orbital analysis that has been carried, in terms of computation of the inclination, eclipse duration, X and S band antenna contacts duration, beta angle variation and semimajor axis variation are shown in Fig. 7. All the proposer heights are feasible for the mission requirements.

2.3.2. Telemetry, Tracking and Command

SPEC Telemetry, Tracking and Command (TT&C) subsystem shall guarantee adequate performances in transmitting the acquired data and in receiving commands from the Ground Stations. The subsystem is composed of a

Table 2: Downlink budget parameters

Parameter	Value
Orbit height	500 km
Elevation	5 deg
Transmission band	S
S/C antenna	patch antenna
GS antenna	10 m parabolic reflector
Modulation	OQPSK
Data rate	10 Mb/s
BER	$< 10^{-6}$
Forward Error Correction (FEC)	Turbo Code Block Size 8920 Rate 1/2

S-Band transceiver, to allow a high data rate, and a low gain patch antenna, to reduce the spacecraft pointing requirements during data transmissions. A UHF transceiver and a monopole antenna shall be in charge for Telemetry and Command transmission. In order to avoid data corruption or the reception of erroneous commands, the Bit Error Rate (BER) shall be equal at least to 10-6. To decrease the needed Energy per bit (Eb/N0), Forward Error Correction (FEC) with Turbo Codes shall be implemented. This allows a very low Eb/N0 threshold that compensate the low available transmission power on board, enabling high data rate transmission to downlink several payload images in a single passage over a GS. The SPEC link budgets, shown in Table 3 for the downlink and Table 5 for the Uplink, take into account a Worst Case Scenario during the lowest visible pass over the ground station for the highest orbit, with the parameters showed in Table 2 for the downlink and in Table 4 for the Uplink. Environmental thermal noise has been calculated following International Telecommunication Union (ITU) recommendation [15].

2.3.3. Ground Segment

SPEC S-band ground segment is composed of two ground stations, one in the Centro di Geodesia Spaziale in Matera, Italy, and one in Luigi Broglio Space

Table 3: Downlink budget

Feature	Symbol	Value	Unit
RF output	P_0	0	dBW
S/C line loss	L_l	0.5	dB
S/C antenna gain (with pointing loss)	G_t	3	dBi
Space loss	L_p	165.65	dB
Ionospheric and atmospheric losses	L_z	2.1	dB
GS antenna pointing loss	L_θ	0.5	dB
GS antenna figure of merit	G_r/T	20	dBi
GS line loss	L_{lr}	1.5	dB
Data rate	R	70	dBHz
E_b/N_0	E_b/N_0	11.35	dB
E_b/N_0 threshold with FEC		1.6	dB
Link margin		9.75	dB

Table 4: Uplink budget parameters

Parameter	Value
Orbit height	500 km
Elevation	5 deg
Transmission band	UHF
S/C antenna	Monopole 1/4 λ
GS antenna	Yagi circular polarization
Data rate	9600 b/s
BER	$< 10^{-5}$
Forward Error Correction (FEC)	Convolutional R=1/2 K=7 & Reed Solomon (255,223)

Table 5: Uplink budget

Feature	Symbol	Value	Unit
RF output	P_0	14	dBW
GS line loss	L_{lr}	1.5	dB
GS antenna gain	G_t	15	dBi
pointing loss GS	$L_{\theta t}$	0.5	dB
Space loss	L_p	152	dB
Ionospheric and atmospheric losses	L_z	2.5	dB
Polarization loss	L_P	3	dB
S/C antenna gain (with pointing loss)	G_r	-1	dBi
Effective noise temperature	T_s	26	dBK
Line loss	L_{lr}	0.5	dB
Data rate	R	39.8	dBHz
E_b/N_0	E_b/N_0	30.8	dB
E_b/N_0 threshold with FEC		7.8	dB
Link margin		23	dB

Center in Malindi, Kenya. Both GS are owned by the Italian Space Agency. The GS are equipped with high gain parabolic reflector that shall reduce the transmitted power from the CubeSat thanks their high Figure of Merit (G/T). Telemetry and command shall be transmitted in UHF-band through the S5Lab Urbe Airport GS.

2.3.4. Electric and Power

SPEC Electric and Power Subsystem (EPS) shall provide the required power to all subsystems during both sunlight and eclipse condition in order to ensure their in orbit operations. The EPS is composed of a Power Control Unit (PCU), a Lithium Ion (Li-Ion) battery pack and several triple junction solar panels mounted on all the faces of the CubeSat except for one with the payload that shall never be pointed to the Sun. Commercial Off The Self (COTS) triple junction solar panels provide up to of 2.4W per each 1U surface, allowing the sustainability of the mission even if only the 2U face of the CubeSat is lit by the Sun. Even in End Of Life (EOF) condition the daily energy budget is positive as shown in Table 6. The duty cycle of subsystems shall be optimized to avoid battery Depth of Discharge (DoD) above 20% to allow enough battery lifetime to sustain the mission. In particular for the payload data downlink to ground which is the most demanding in term of power consumed. The subsystem shall provide latch-up protection needed for space applications due to environmental ionizing radiation from cosmic rays or solar flares. The subsystem shall ensure battery pack passivation at the end of the mission lifetime to be compliant to the Space Debris Mitigation guidelines [16].

2.3.5. Thermal Control

SPEC Thermal Control subsystem shall maintain all components of the CubeSat within their operative temperature range during the whole mission lifetime. The most thermally critical components are the solar panels, that sustain the greatest thermal gradients during dawn and dusk conditions, and the battery pack, that has the narrower operative temperature range, usually be-

16

Table 6: EOL Daily Energy Budget

Component	Minutes	Duty Cycle	Power [W]	Consupmtion [Wh]
Payload	30	2.04%	-10	-5.10
OBDH	1472	100.00%	-0.15	-3.68
ADCS	60	4.08%	-3	-3.00
GPS	20	2.04%	-1.2	-0.60
TTC-RX	1472	100.00%	-0.23	-5.64
TTC-TX	32	2.17%	-5	-2.67
BEACON	28	1.90%	-2.8	-1.31
EPS	1472	100.00%	-0.16	-5.95
Solar Array	912	61.96%	2.2	+33.44
Daily Margin				+5.49

tween -10 C and +45C. The thermal control system is mainly passive consisting in the usage of heat bridges and heat sinks to avoid overheating of the most dissipative components and insulating material to reduce thermal fluxes to the optical payload. Active components as heaters shall be included, aimed at controlling the battery pack temperature. The optical payload shall be thermally isolated from the rest of the structure to reduce thermal cycling and stress due to the rapid temperature variation during the entry and exit from eclipse [17].

2.3.6. Attitue and Determination Control

Pointing requirements are very strict for space observations, therefore SPEC Attitude and Determination Control (ADCS) is a key subsystem for the performance of the mission. As describe in the mission paragraph, SPEC optics FOV is around 0.6 degrees. To maintain the targeted binary system inside the FOV, the ADCS shall assure a pointing accuracy of at least 0.3 degrees and shall maintain it for an sensor exposure time of around 10 seconds. To obtain the required pointing accuracy SPEC is equipped with a star tracker, a fine sun sensor, a low noise magnetometer and a GPS receiver to accurately determine its position in space. A set of reaction wheels and magnetorquers are equipped

17

to perform fine pointing. To perform wheels desaturation SPEC shall use the magnetorquers. To reduce the space allocation, low encumbrance COTS shall be selected. Several companies [18, 19] offer reaction wheels that occupy less than 1U and magnetorquers that are integrated on the back of solar panels.

3. Conclusions and future perspectives

SPEC CubeSat mission shall enhance the methods for observing binary stellar systems with a low cost space-born platform and shall verify the capability of CubeSat for future optical missions. The mission is based on a 6U Cubesat, limiting the costs, the mass and the volume of the scientific and standard satellite components. The previously shown results demonstrate the theoretical feasibility of a Cubesat based mission for astronomical purposes focused on binary systems observation. The requirements imposed by the selected targets, according to the star distance, magnitude, and angular separation between the system members are completely fulfilled by the designed system, achieving high angular resolutions below 5 arcseconds. Such a fine angular resolution can guarantee the observability of the scientific targets with a compact optical system.

References

[1] A. J. Burgasser, I. N. Reid, N. Siegler, L. Close, P. Allen, P. Lowrance, J. Gizis, Not Alone: Tracing the Origins of Very-Low-Mass Stars and Brown Dwarfs Through Multiplicity Studies, Protostars and Planets V (2007) 427–441arXiv:astro-ph/0602122.

[2] C. Bergfors, W. Brandner, M. Janson, S. Daemgen, K. Geissler, T. Henning, S. Hippler, F. Hormuth, V. Joergens, R. Köhler, Lucky Imaging survey for southern M dwarf binaries, A&A 520 (2010) A54. `arXiv:1006.2377`, `doi:10.1051/0004-6361/201014114`.

[3] B. Riaz, J. E. Gizis, J. Harvin, Identification of New M Dwarfs in the Solar Neighborhood, AJ 132 (2006) 866–872. `arXiv:astro-ph/0606617`, `doi:10.1086/505632`.

[4] I. Baraffe, G. Chabrier, T. S. Barman, F. Allard, P. H. Hauschildt, Evolutionary models for cool brown dwarfs and extrasolar giant planets. The case of HD 209458, A&A 402 (2003) 701–712. `arXiv:astro-ph/0302293`, `doi:10.1051/0004-6361:20030252`.

[5] D. G. York, J. Adelman, J. E. Anderson, Jr., S. F. Anderson, J. Annis, N. A. Bahcall, Bakken, et al., The Sloan Digital Sky Survey: Technical Summary, AJ 120 (2000) 1579–1587. `arXiv:astro-ph/0006396`, `doi:10.1086/301513`.

[6] S. Daemgen, N. Siegler, I. N. Reid, L. M. Close, Discovery of Nine New Companions to Nearby Young M Stars with the Altair AO System, ApJ 654 (2007) 558–569. `arXiv:astro-ph/0609356`, `doi:10.1086/509109`.

[7] A. L. Kraus, L. A. Hillenbrand, The Stellar Populations of Praesepe and Coma Berenices, AJ 134 (2007) 2340–2352. `arXiv:0708.2719`, `doi:10.1086/522831`.

[8] F. Santoni, URSA MAIOR: a One Liter Nanosatellite Bus for Low Cost Access to Space, in: IAF abstracts, 34th COSPAR Scientific Assembly, 2002, p. 204.

[9] L. Arena, F. Angeletti, F. Curian, G. De Zanet, R. Gradini, A. Pellegrino, Thermal and mechanical design and test campaign results of a single-piece structure for the ursa maior nanosatellite.

[10] F. Piergentili, M. Balucani, R. Crescenzi, J. Piattoni, F. Santoni, B. Betti, F. Nasuti, M. Onofri, Mems cold gas microthruster on ursa maior cubesat 9 (2013) 7137–7143.

[11] P. Seitzer, J. Cutler, F. Piergentili, F. Santoni, L. Arena, T. Cardona, H. Cowardin, C. Lee, S. Sharma, LEDsats: LEO CubeSats with LEDs for Optical Tracking, in: Advanced Maui Optical and Space Surveillance Technologies Conference, 2016, p. 115.

[12] A. Pellegrino, P. Seitzer, F. Piergentili, F. Santoni, J. Cutler, T. Cardona, P. Marzioli, G. Cialone, S. Masillo, et al., LEDSAT: in-orbit demonstration mission for led-based cluster launch early identification and improved leo surveillance.
URL http://iafastro.directory/iac/paper/id/41050/summary/

[13] K. Ward-Duong, J. Patience, R. J. De Rosa, J. Bulger, A. Rajan, S. P. Goodwin, R. J. Parker, D. W. McCarthy, C. Kulesa, The M-dwarfs in Multiples (MINMS) survey - I. Stellar multiplicity among low-mass stars within 15 pc, MNRAS 449 (2015) 2618–2637. arXiv:1503.00724, doi: 10.1093/mnras/stv384.

[14] F. van Leeuwen (Ed.), Hipparcos, the New Reduction of the Raw Data, Vol. 350 of Astrophysics and Space Science Library, 2007. doi:10.1007/ 978-1-4020-6342-8.

[15] International Telecommunication Union (ITU), Recommendation p.372 for radio nosie (2016).
URL https://www.itu.int/rec/R-REC-P.372/en

[16] UNITED NATIONS, Space Debris Mitigation Guidelines of the Committee on the Peaceful Uses of Outer Space (2010).
URL http://www.unoosa.org/pdf/publications/st_space_49E.pdf

[17] D. G. Gilmore, Spacecraft Thermal Control Handbook: Fundamental technologies, Aerospace Press, 2002.

[18] GOMSPACE: a company offering compact ADCS based on reaction wheels.
URL `https://gomspace.com/Shop/subsystems/adcs/nanotorque-gsw-600.aspx`

[19] Cubesatshop: a company offering compact ADCS based on reaction wheels.
URL `https://www.cubesatshop.com/product/mai-400-adacs/`